Construction and Building Materials 398 (2023) 132496

Contents lists available at ScienceDirect

Construction and Building Materials

journal homepage: www.elsevier.com/locate/conbuildmat

Sustainable mixes for 3D printing of earth-based constructions

Flora Faleschini *, Daniel Trento, Maryam Masoomi, Carlo Pellegrino, Mariano Angelo Zanini

Department of Civil, Environmental and Architectural Engineering, University of Padova, via F. Marzolo 9, 35131 Padova, Italy

ARTICLE INFO

Keywords:
3d printing
Additive manufacturing
Cob
Earth materials
Sustainability

ABSTRACT

This work shows the results of an experimental campaign aimed at selecting earth-based sustainable mixes for 3D printing. For this scope, 18 mixes were realized, varying the types of components, their amount in the mix and the hydration rate. Specifically, the analyzed components are locally-available soil, hydraulic lime binder, unaltered rice husk, shredded rice husk, marble waste dust, municipal solid waste incinerator bottom ash, silica sand, and natural fibers, including jute, coconut, sisal and goat hair. Each mix was tested in terms of printability via a preliminary test, then compressive and flexural strength were measured at 28 days, and lastly shrinkage was experimentally investigated. Among the analyzed mixes, two of them were further optimized to realize some 3D printed blocks and verify their effective printability in a full-scale construction project. Results demonstrated that it is possible to obtain mixes with relatively good strength and limited shrinkage. According to a multi-criteria efficiency evaluation carried out here, it was possible to evaluate which mix performs best, considering the mechanical performance, the economic price and the carbon footprint of each mix. Particularly, a mixture containing lime as binder and sisal as long fibers allows attaining a compressive strength of 1.26 MPa, embodied carbon of about 0.05239 kgCO_2eq/kg with a selling price of 0.137€/kg, being the most efficient one. Instead, the optimized mixture used for real-scale printing achieved 11.04 MPa of compressive and 1.26 MPa of flexural strength.

1. Introduction

Construction accounted for 37% of global greenhouse gas emissions in 2020 [1], and 25% of solid waste generated in the world [2]. Given the pollution associated with the construction sector, finding sustainable methods and materials to reduce the negative impacts of this industry on both environment and society is the need of the hour. For this scope, huge efforts are paid by the scientific community to study alternative construction materials that should at least replace in part the traditional ones. In this context, the research in terms of developing new binders with low clinker content [3–5], geopolymer-concretes [6–10], recycled aggregates from construction and demolition waste [11–15], slags [16–18] and other hazardous waste [19–21] is worth being mentioned. However, great efforts are being made also in terms of finding sustainable construction technologies, able to reduce the generated waste in the construction process, limiting the use of formworks and wooden molds. In this context, additive manufacturing (AM) processes can surely represent a viable solution to improve the efficiency of the construction industry [22]. In fact, through this technology, costs, time and impacts linked to formwork building are almost avoided at all.

Literature on 3D printing (3DP) of concrete has been sensibly increased in the last years [23–30], highlighting how the economic and environmental issues of large-scale 3DP of concrete structures needs still to be optimized: although the highly reduced cost of labor and formworks, printable materials are not inexpensive at all, compared to ordinary concrete. The same applies for their environmental impacts, since generally the content of cement and some additions such as silica fume are higher than in ordinary concrete [31], this being necessary to allow the required rheological properties and printability. Thus, recalling the poor sustainability of ordinary Portland cement compared to other alternatives, the recent literature has focused also on rehabilitating traditional earth constructions, which can be suitably adopted at least for some construction typologies and are already widely diffused in large areas of the world (see Fig. 1, [32]). Thanks to some exemplary recent projects (e.g., the hospital designed by Renzo Piano in Uganda for the ONG *Emergency*, which main walls are made of rammed earth), the perception of earth architecture has evolved significantly in the recent years, to reflect different environmental, technological and cultural contexts [33]. Earth blocks have recently been subject to national rules and standards set by several countries, namely New Zealand (NZS

* Corresponding author.
E-mail address: flora.faleschini@dicea.unipd.it (F. Faleschini).

https://doi.org/10.1016/j.conbuildmat.2023.132496
Received 16 March 2023;
Available online 19 July 2023

D4298 [34]) and New Mexico Earthen Building Code [35]. In Italy, WASP 3D printed the first actual full-size earth structure in 2016, this being the key milestone in the valorization process of traditional construction techniques [36]: since that moment, the attention to this concept of construction, with locally-available materials, that promotes the sustainability and the aesthetic of the 3DP process, increased extremely.

Among the different earth-based constructions, there are various techniques that evolved in time, depending on how the materials are mixed and on the construction process. Specifically, there are both "wet" and "dry" methods: the former uses the earth material in a plastic state, and among them it is worth mentioning the adobe, cob, wattle, daub and earthen plaster; the latter includes techniques such as the compressed earth block and the rammed earth. Most of them allow to realize load-bearing elements, are characterized by a very low embodied energy and responsible for limited environmental impacts [37] and generally they have very good thermic and insulation properties [38,39]. With a perspective of using earth-based materials in a 3DP process, the wet methods are the most suitable, and for this reason, adobe and cob techniques are the most investigated ones. They differ from the construction method type: adobe refers to build walls using sun-dried blocks; instead, building monolithic walls with plastic earth-mixes is known as cob [40]. From a material point of view, adobe and cob are made by the same constituents in their original conception, i.e., subsoil, straw and water. Between adobe and cob, this last stands out as the closest to 3DP of earth structures since both methods deposit successive layers of mixture to construct a structure, and its compressive strength is generally less than 2 MPa [41]. However, the traditional mix design of cob mixtures requires low water content and high density, thus hardly meeting the requirements for printability [42]. For this reason, an upgrade of this traditional technique is necessary to satisfy the demands of extrudability and buildability for 3DP.

Designing a thixotropic substance that can be easily extruded during the printing process while preserving its original shape after deposition is the key problem in the development of a printable mixture [43]. Reyes et al. [44] changed the typical cob mix design to make it compatible with 3DP technology, proposing a new formulation made by 30% of sub-soil and 15% silica sand, 15% of straw, 18% water, and 22% clay. To reduce the viscosity during the printing process, Gomaa et al. [33] recommended water content ranging between 23 and 25%, with 2% of straw. Alqenaee and Memari [45] proposed a mixture made with 49% clay, 24.2% water, 15.3% sand, 10% lime, and 1.5% straws. Instead of straw, Ferretti et al. [46] used unaltered and shredded rice husk in two different mixtures and lime as a stabilizer, to realize 3D printed earth blocks. Perrot et al. [47] prepared a mixture by adding alginate to the earth, composed of clay particles, quartz, kaolinite, illite and smectite, with water content of 45%. Silva et al. [48] realized instead a mixture for 3DP with 5% potato starch gel and 1% sisal fibers, whereas the earth was composed of 4% by weight of medium sand, 30% of fine sand content, 41% of silt sizes, and 25% clay.

Other key aspects related to 3D printed mixes are the minimum required mechanical performances, asked to the material to stand up under its own weight and that of the upper layers, a sufficient bond between further layers, and the necessity to limit the shrinkage. The mechanical properties of adobe, cob and more generally speaking, earth-based materials, highly depend on water content inside the mixture and on ambient moisture [47].Water content also affects mixtures' flowability, a key property that governs the printability of the mix, which should be extruded from the nozzle to print efficiently [45]. So, the first important challenge is to find the optimum volume of water in the mixture to meet both requirements of strength gain and extrudability. Concerning specifically strength development, the early strength of the 3DP mixture in its fresh state is important since the extruded mixture should withstand its own weight and the weight of subsequent layers. In this regard, the adhesion between extruded layers needs an adequate investigation, since poor interlayer bond is one of the primary issues that may cause the failure of 3DP blocks and structures [49]. While numerous studies were carried out on the effect of various factors on the interlayer bond in 3DP cementitious materials [49–51], to the knowledge of the authors, no studies focused on the same aspect in earth-based 3DP materials. Shrinkage requires also particular attention, since it can run the risk of developing cracks in 3DP buildings, and its phenomenon is characterizing the behavior of soil-based materials. For these materials, shrinkage is defined as the specific volume change of soil relative to its water content and is mainly due to clay swelling properties under water evaporation [52]. Type and content of clay affects the overall shrinkage of soil, and thus the vulnerability of earth-based buildings to shrinkage is highly dependent on their mix design. Ferretti et al. [46] measured shrinkage strains in both 3DP and normally casted blocks, realizing that there is no significant difference between them. In other words, the printing process does not negatively affect shrinkage behavior in earth-based buildings [45].

Given the above context, this work aims to evaluate the feasibility of adopting new earth-based mixes for 3D printing. The main goal is to maximize the content of recycled and natural materials inside the mix, achieving some minimum target performances in terms of mechanical strength and shrinkage. Printability is evaluated empirically with a simple test method at the lab-scale. Once the most promising mixes were identified, one of them was then optimized and a 3D printing test was carried out and some real-scale blocks were effectively fabricated. As elements of novelty, we investigated the feasibility of mixing together different residues and natural materials, which are locally-available in huge quantities in our region. For this scope, marble dust, rice husk and municipal solid waste incinerator bottom ash were used to partially

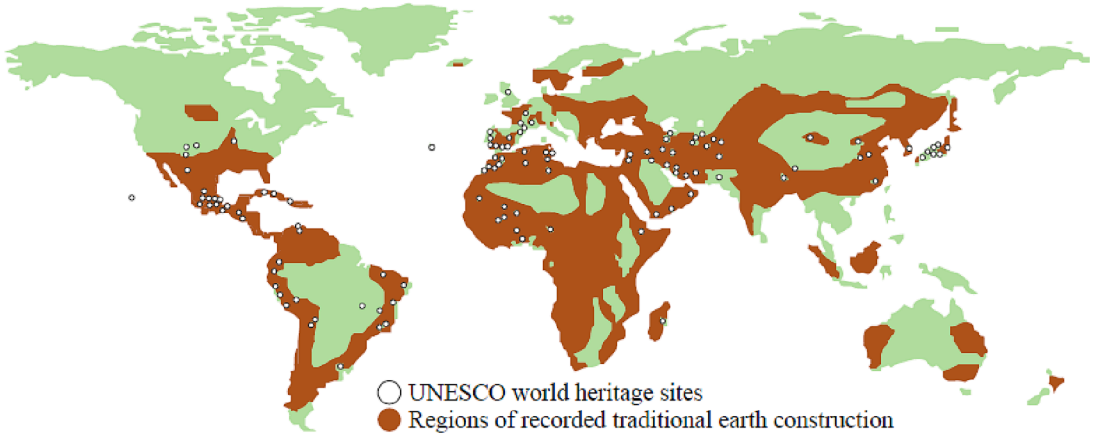

Fig. 1. Diffusion of traditional earth-based construction adapted from [32].

substitute the binder types, both cement and lime. Furthermore, the adoption of different types of natural fibers was experimentally tested, to evaluate their effect in limiting shrinkage deformation. Another element of novelty is the validation in a real-scale 3D printer, using the same technology adopted for the actual construction process of large earth-based buildings: the results achieved in this work clearly indicate the feasibility of designing a fully sustainable earth-based mix with sufficient mechanical strength and low shrinkage deformability to allow printing a full-scale structure.

2. Materials and methods

2.1. Materials

To realize the preliminary 3DP mixes, the following materials were used: locally available soil (So), sand (Sa), lime (NHL), rice husk (RH), municipal solid waste incinerator bottom ash (MSWI BA), marble dust (MD), potable water (W). A cement type CEM II/B-LL 32.5R according to [53] was also used in some mixes. Rice husk, MSWI BA and marble dust were used to reduce the amount of lime in the mix, thus making it more sustainable. Further, the use of natural fibers was also investigated, and among them jute (JF), coconut (CF) and sisal fibers (SF) were tested, other than goat hair (GH). The adoption of such materials aims ideally to substitute the straw, which is the fiber typically used to fabricate cob mixture. In fact, straw can clog the nozzle of 3D printers or block inside the extrusion system, because of its size [45]. The materials used to cast the experimental mixes are shown in Fig. 2.

The collected soil comes from the region around Padova, Italy. The grains size distribution was determined through sieve analysis, according to [54–55], and the resulting soil fractions distribution is given in Table 1. In addition, Atterberg limits were evaluated according to [56], and are listed in Table 2, where liquid and plastic limits, the plasticity

Fig. 2. Materials used for the preliminary 3DP mixes: a) Soil; b) Sand; c) Lime; d) Rice Husk (RH); e) Shredded Rice Husk (SRH); f) Municipal Solid Waste Incinerator Bottom Ash (MSWI BA); g) Marble Dust (MD); h) jute fibers (JF); i) coconut fibers (CF); j) sisal fibers (SF); k) goat hair (GH).

Table 1
Percentage of fine and coarse aggregates in the soil.

Soil	Silt + Clay	Sand	Gravel
Percentage	68.24%	28.8%	2.96%

Table 2
Physical properties of the materials used for the 3DP preliminary mixes.

	Soil	
Atterberg limits (%)	Liquid Limit (W_L)	22
	Plastic Limit (W_p)	16
	Plastic Index (PI)	6
Density (kg/m^3)	Loose bulk density	1038.75
	Compacted bulk density	1324.75
	Sand	
Density (kg/m^3)	Air-dry density	2644
	Apparent relative density	2470
	Saturated surface dry density	2530
	Water absorption (%)	2.71
	Rice Husk	
Density (kg/m^3)	Loose bulk density rice hush	95
	Loose bulk density shredded rice husk	475
	Municipal Solid Waste Incinerator Bottom Ash	
Density (kg/m^3)	Air-dry density	2667
	Apparent relative density	2057
	Saturated surface dry density	2286
	Water absorption (%)	11
	Marble Dust	
Density (kg/m^3)	Air-dry density	2300
	Apparent relative density	2107
	Saturated surface dry density	2570
	Water absorption (%)	4.5

index and soil bulk density are shown. According to [56], the soil indexes and particles size distribution are consistent with those of a low-plasticity, well-graded silty clay. To make the soil suitable for 3DP, an extra amount of sand was added to the soil. Sand type is a natural limestone provided by a local quarry near the city of Padova, with a 0–4 mm grading (see Fig. 3), which density is listed in Table 2.

The lime used in this work is a natural hydrated lime NHL 5, according to the nomenclature given by [57]. It is obtained from the calcination of marly limestones, rich in silica and alumina, in vertical

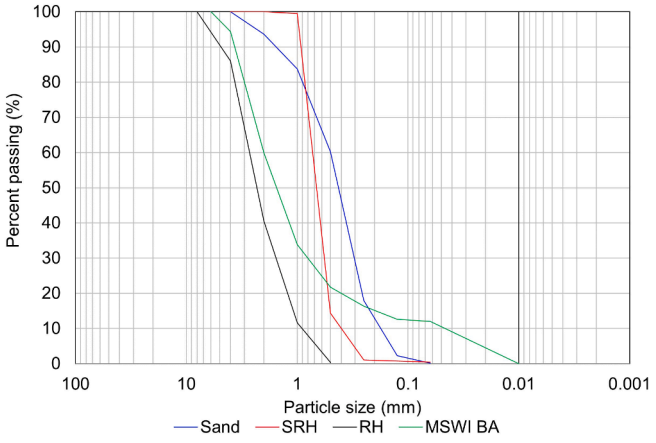

Fig. 3. Particles grading curve of sand, rice husk (RH), shredded rice husk (SRH) and MSWI BA.

layered kilns, with a slow process and at temperatures around 1000 °C. Lime properties, as declared by the producer, are displayed in Table 3, together with those of the cement. Cement type is CEM II/B-LL 32.5R type, according to the definition of [53], which is a Portland-limestone cement with high content of limestone (up to 35%).

Then, a set of materials used to partially replace the ordinary binder is investigated. All these materials are locally-available and are waste that need to find a suitable alternative compared to their landfilling. Among them, rice husk was the first tentative, which was used both as received (RH) and shredded (SRH). Rice husk was found to be highly reactive when combusted and properly ground ash is obtained, due to its high content of reactive silica [58–59]. However, the presence of amorphous silica is found in the rice husk too, which can give rise to pozzolanic effect and induces benefits both on the mechanical strength and durability of cement-based materials [60]. In the first case (RH), the grain size dimension makes it more similar to a fiber, but with a shorter length than straw; in the second case (SRH), it can be thought more as a fine natural compound, with potentially some pozzolanic activity. The particles size distribution of the two rice husk types are shown in Fig. 3. The average length l of the rice husk is 7.65 mm, with an average diameter d of 2.575 mm evaluated according to [61]; thus, the aspect ratio is $l/d = 2.971$. The dimensions were evaluated through microscope measurements. The loose bulk density of rice husk, evaluated again according to [61], and that of shredded rice husk, are listed in Table 2. The water absorption of rice husk was assessed with the method proposed by [62]: dried samples of rice husk weighing 5 g were placed in tulle bags and submerged in water for 15 min, 4 h, and 48 h. Each time, the tulle bags were submerged, they were drained and weighed. Most of the water is absorbed in the first 15 min (about 65%), and in the next 4 h it attained the 100% of the initial weight. In terms of morphology and chemical composition, rice husk was analyzed via a scanning electron microscopy (SEM) with secondary electron (SE) mode, and Energy Dispersive X-ray Spectroscopy (EDS) analysis was carried out. Fig. 4a shows the cellular morphology of the rice husk, whereas the main composition evaluated both on the inner and outer surface of the particles was made of silicon oxides. As a minor constituent there was carbon, followed by sodium and potassium in traces. It should be

Table 3
Lime and cement properties.

Characteristics – Lime	Type NHL 5	Requirements EN 459-1: 2015 [57]
Color	Hazelnut-pink	–
Compressive strength – 7 days	>2 MPa	>2 MPa
Compressive strength – 28 days	>5 MPa	≥5 and ≤ 15 MPa
Time to start setting	>1 h	>1 h
Time to finish setting	≤ 11 h	≤ 15 h
Residual fineness at 0.09 mm	<10%	≤ 15%
Residual fineness at 0.2 mm	<0.5%	≤ 2%
Volume stability	≤ 0.5 mm	≤ 2 mm
SO_3 sulfate content	<1%	≤ 2%
Free lime content	>15%	≥15%
Apparent density	0.7 g/cm^3	–
Characteristics – Cement	**Type II/B-LL 32.5R**	**Requirements EN 197–1: 2011 [53]**
Compressive strength – 2 days	≥10 MPa	≥10 MPa
Compressive strength – 28 days	≥32.5 MPa	≥32.5 MPa
Setting time	≥75 min	≥75 min
Expansion	≤10 mm	≤10 mm
SO_3 sulfate content	≤3.5%	≤3.5%
Chloride content	≤0.1%	≤0.1%

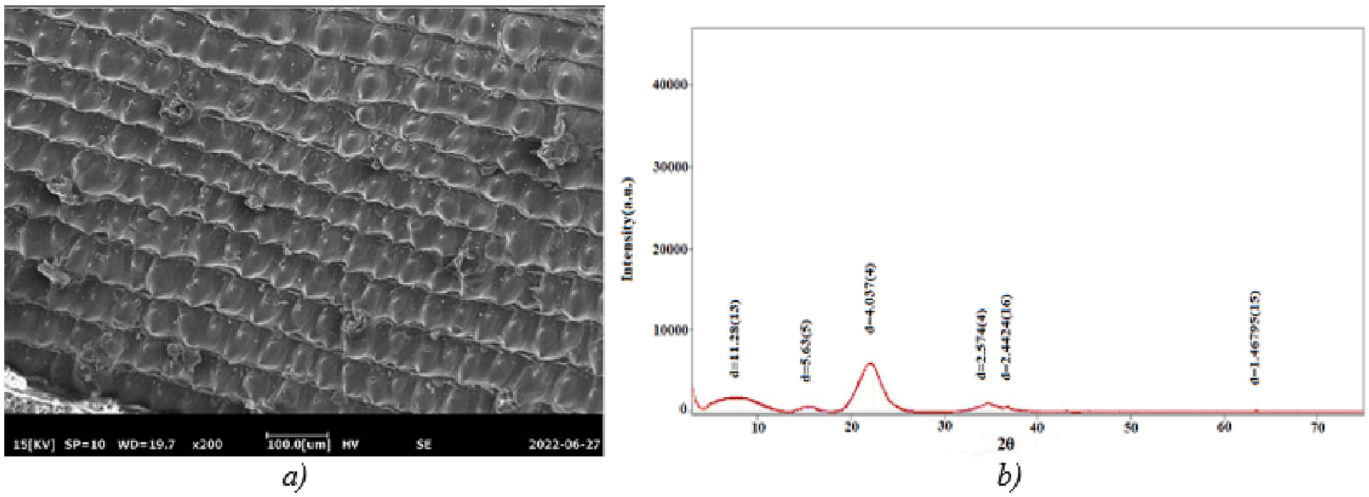

Fig. 4. a) SEM-SE photo of the inner structure of the rice husk; b) XRD pattern of the rice husk.

recalled that the formation of silicon–oxygen– silicon bridge bonds (Si–O–Si bonds) is fundamental for geopolymerization process, as well as a source of reactive silica. The major compounds of the rice husk are polysaccharide organics, such as cellulose, hemi-cellulose and lignin, as expected. Particularly, from X-Ray Diffraction (XRD), it is possible to distinguish the presence of cellulose which, differently from hemicellulose and lignin that are amorphous, has a crystalline structure. Fig. 4a depicts the detail of the internal surface of the rice husk, whereas Fig. 4b clearly shows the presence of the peaks around $2\theta = 16°$, 22°, and 35° that are typical of cellulose natural fibers [63].

The second material analyzed is municipal solid waste incinerator bottom ash (MSWI BA), used here as an alternative sustainable stabilizer for the earth mixtures. MSWI BA may be characterized by certain reactivity, depending on their composition [64], this material was provided by a waste treatment plant near Verona. The particles size distribution is shown in Fig. 3: note that the powder content is very high, about 12% of the particles have a dimension less than 0.063 mm. However, the particles size can reach dimensions as high as 4 mm. The physical properties are instead listed in Table 2, where densities and water absorption, evaluated according to [65] are listed. Concerning the chemical composition, evaluated by means of X-Ray Fluorescence (XRF) spectroscopy, the main constituents are Ca, Si, Al, Fe and Mg oxides; particularly, $SiO_2 + Al_2O_3 + Fe_2O_3$ content is about 42.4%. A micrograph from SEM collected in the backscattered electron mode (BSE) is shown in Fig. 5a, which allows to identify through the gray-scale of colors, a wide range of compounds present in the ash. The complex mineralogy was instead characterized by means of XRD test, which results are shown in Fig. 5b, that allows to identify the most relevant crystalline phases, made by quartz, calcite, gehlenite, magnetite, wuestite, mayenite, larnite and then calcium sulfate tetrahydrate. In the XRD spectrum, it is possible to detect a main hump between 25° and 35° 2θ, representing an amorphous phase.

Lastly, the marble dust used in this work comes from a limestone mud taken from the cutting of blocks from the extraction area of the Berici Hills in Vicenza district, very famous for the so-called "Pietra di Vicenza", used by Andrea Palladio in the XVI Century and in other historical buildings. This material is currently considered as a waste according to the Italian law and it needs urgently to be recycled to avoid its landfilling in the area close to Padova. The material appears as a white paste which humidity is in average 4.5%. The physical properties are listed in Table 2. After drying in oven at 105 °C for 24 h, the grain size distribution is obtained, and it is made up of very fine particles, with d_{90} less than 20 μm, as shown in Fig. 6. The semi-quantitative composition, evaluated with the EDS device on micrographs obtained with the SEM, is overall homogeneous, revealing mostly Ca oxides: the material is a mixture of larger $CaCO_3$ and smaller $Ca(OH)_2$ crystals, as shown in

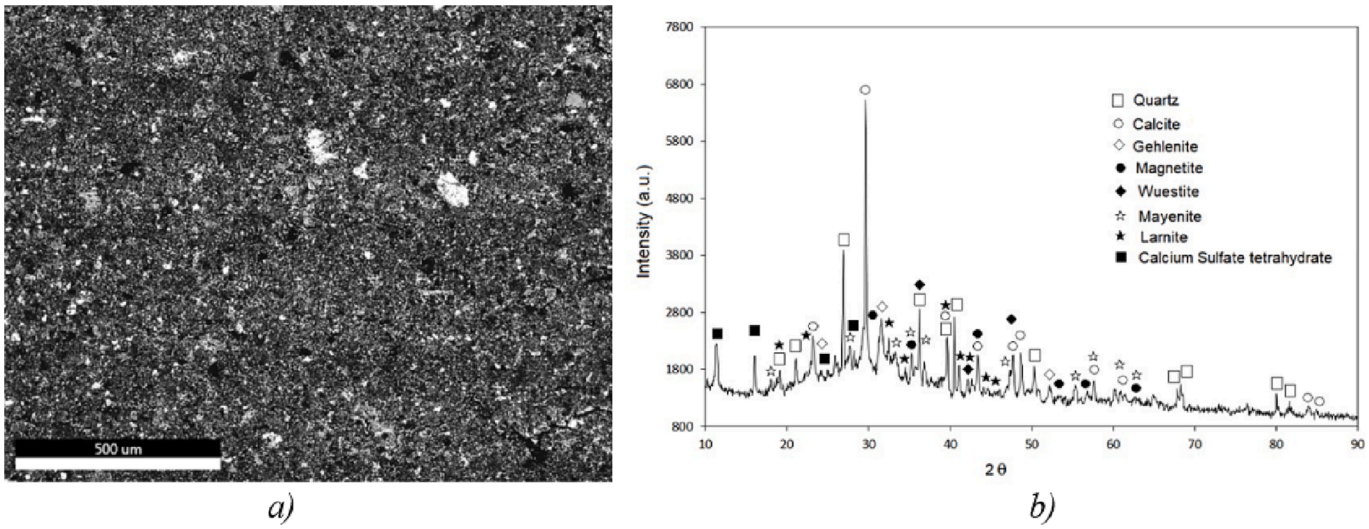

Fig. 5. a) SEM-BSE photo of the MSWI-BA; b) XRD pattern of the MSWI-BA.

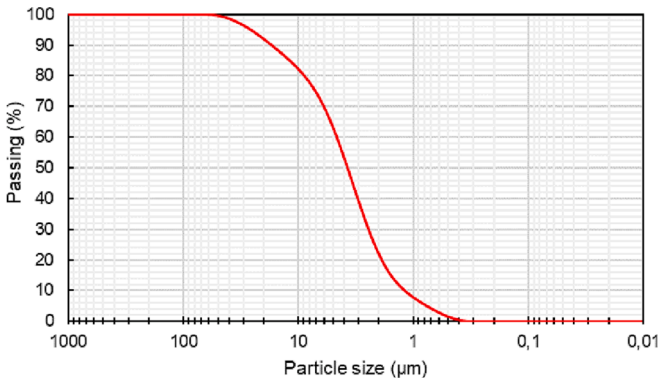

Fig. 6. Particles grading curve of the marble dust.

Fig. 7a. When simply exposed to air, the $Ca(OH)_2$ crystals quickly carbonate, forming calcite crystals only, as shown from the XRD pattern in Fig. 7b, taken on a sample of air-dried particles after 2 weeks from the collection at the plant.

As previously recalled, the use of natural long fibers in earth mixtures is quite common, as they allow to reduce shrinkage and improve tensile strength. In this experimental investigation, all the long fibers are characterized by the same average aspect ratio $l/d = 50$, but with different length and diameter. The fiber properties are shown in Table 4.

The use of such different materials is justified because most of them are widely available in North-Eastern Italy and are currently classified as waste according to the Italian legislation. For instance, the soil and the sand were provided from quarries near the city of Padova, while Municipal Incinerator Bottom Ash and marble dust are by-products provided by local factories. Several natural fibers were used in this paper, most of them were already employed in previous works [32,43]. The preparation of mixtures with different fiber types has the main scope to assess the properties of each one in earth-based mixtures.

2.2. Mix design

To design a suitable 3DP mix, two sets of tentative mixtures were prepared, based on the available knowledge both on ordinary and 3DP cob: the first set of mixes does not contain any fiber, whereas the second is made with the different types of natural fibers analyzed in this work. Only once the best mix was identified, it was further optimized in terms of constituents' properties and mix proportions and some real-scale 3DP blocks were realized, see Section 4.

First, the variables that were identified as most influencing the final properties of an earth-based mix are the water and binder content, and type. According to ASTM E2392-M10 [66], in fact, strength and durability of the finished product are substantially affected by the mixing time and quality of the combination of earth and water. In conventional earth-based material preparation, the water demand is significantly increased by the fiber addition, too. As an indicative number, Palumbo et al. [67] showed that using 0 or 2 wt% of corn pitch for plaster preparation can increase the water demand from 17 to 57%.

According to Gomaa et al. [33], a cob mixture should comprise 78% subsoil, 25% water, and 2% fiber by weight. The total content of binders such as cement, lime, or plaster must be less than or equal to 15% of the dry mass of the earth block [45]. There, the amount of fibers in the mixture was 1.4%, similar to ordinary cob; the base soil was blended with silica sand, in a quantity ranging between 18% and 23%, to meet the soil requirements for earth blocks. The water in traditional cob was 20% by mass, but it was found not suitable for 3D printing. Many authors propose to increase this amount up to 24–25%.

Given the above context, the first set of mixes is constituted of 13 mixtures, where the percentage of the different materials varied to find the one characterized by the highest mechanical properties. Particularly, binder type, water content, binder substitution rate with one of the alternative materials (rice husk, MSWI BA and marble dust) are the key variables of the first trials. These mixes are casted without any fibers addition. Fig. 8 depicts the steps to prepare the mixtures, while Table 5 details the mixture proportions. Mixtures from 1-A to 6-A contain cement as binder with a water/binder (w/b) ratio ranging between 1.81 and 2.50, while mixes from 7-A to 13-A contain only natural lime as binder with a w/b ratio between 2.09 and 2.91. Instead, the second set of trials is made of five mixes, where fibers were added. The mix proportions are shown in Table 6, whereas the mixing procedure is the same as that shown in Fig. 8, except for the fibers addition, which was done in the same moment of the rice husk one. The second set of mixtures was prepared using only lime as a binder and a w/b ratio equal to 2.42.

Table 4
Long fibers properties.

Characteristics – Long fibers	Juta fiber	Coconut fiber	Sisal fiber	Goat hair
Average diameter (mm)	1	0.3	0.5	0.2
Average length (mm)	50	15	25	10
Aspect ratio (-)	50	50	50	50

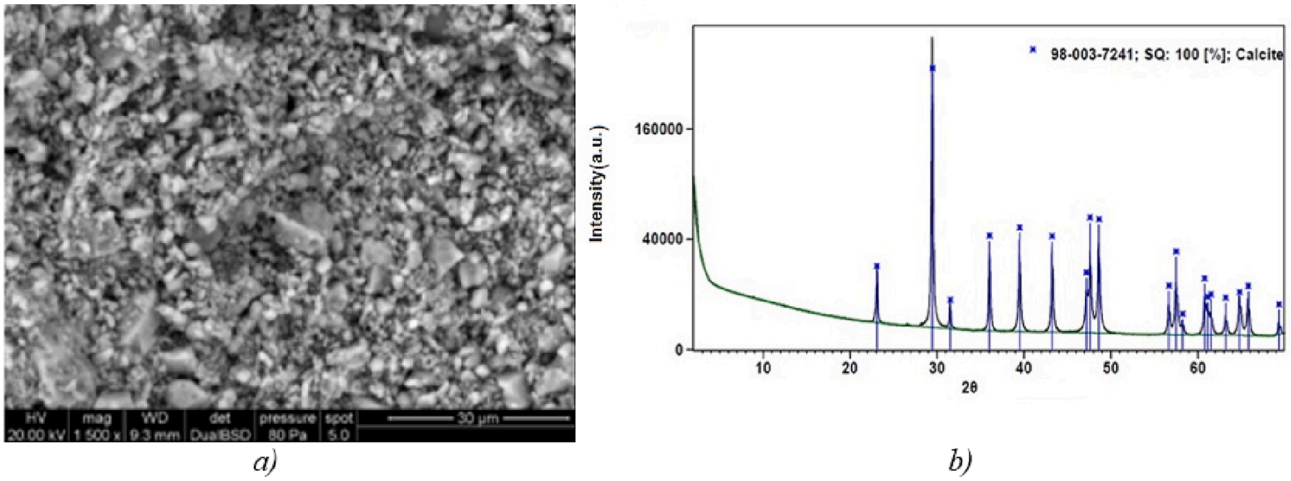

Fig. 7. A) sem-bse photo of the marble dust; b) xrd pattern of the marble dust.

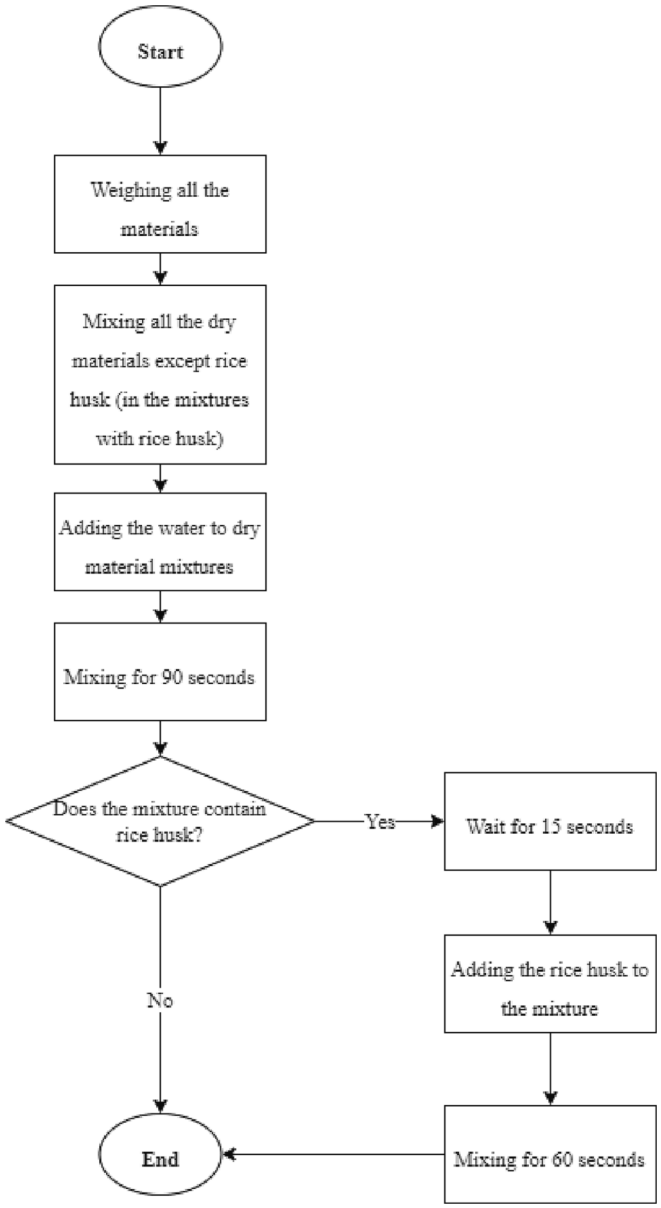

Fig. 8. Experimental procedure for mixture preparation.

2.3. Test methods

For each mixture, three prismatic specimens with dimension 4 cm × 4 cm × 16 cm were casted for the characterization of mechanical properties. After mix preparation, the material was poured into molds and slightly compacted, then the specimens were covered with plastic bags. Five days after casting, the samples were demolded, weighed, and placed in a most room (average temperature 20° C; relative humidity 90%) for curing. The mechanical properties were defined using test procedure typically employed for mortar, as performed by Antunes et al. [62], which reference standard is EN 1015–11:2019 [68]. First, all the specimens were tested in a three-point bending test setup with a span of 100 mm under displacement control at a 0.4 mm/min rate using a universal 25 kN servo-testing machine and the linear voltage displacement transducer (LVDT) of the same testing apparatus. After the flexural test, the remaining specimens were tested in compression using the same loading rate of 0.4 mm/min. It is worth recalling that testing the mixtures, casted following the same procedure shown in Fig. 8, allows to obtain easily reproducible results, independent on the 3D printer apparatus where they may be employed.

The mix extrudability is an important parameter to verify the possible usage in 3D printing equipment. In this context, the authors evaluated the flowability of the fresh mixtures using several sac-a-poche extrusion trials, recognizing that this method is a easy way to simulate very well the extrusion process, but remains empirically-based. The equipment consists in disposable sac-a-poche, its end was closed as provided and it was cutted to the desired width to simulate the proper noozle size of a 3D printer. In our cases, we tested the widths varying from 8 to 20 mm. This test was carried out immediately after completing the procedure described in Fig. 8, i.e., on the fresh material, that was poured into sac-a-poche and squeezed out manually following a track in the prismatic molds. As well known, the pression needed to extrude the fresh material is proportional to the flowability. In some cases, the mixture was too dry to be extruded, indeed the manual pressure was not sufficient to print, and the sac-a-poche breaks easily. In other situations, the water content was too high, and a minimum pressure could extrude too much material. Instead, the shape was preserved when the material was extruded softly thanks to the strong adhesion between layers and the mechanical strength of the base layer. The mixture's buildability indicates that the intervals between layer extrusions were neither too short nor too long [47]. Through this simple empirical procedure, it was evaluated as potentially good to be 3D printed. Furthermore, the ability of a mix to sustain the upper layers, maintaining the original shape, was considered additionally as a factor for a potential goodness to be printed. The procedure followed here is visible in the video-resource attached to the electronic version of this work (Video 1), where a mix characterized by a "good printability" is tested.

To measure the drying shrinkage, mixtures were cast into the same 4 × 4 × 16 cm molds and were removed after 24 h. After that, specimens were cured for 25 days in a standard laboratory climate at a relative humidity of 60 ± 10% and a temperature of 21 ± 2 °C [69]. The shrinkage was determined as the difference between the initial length, i.e., the measured length of specimens immediately after placing the samples in the drying room, and length measurement at specific times 1,

Table 5
First set of mixes (no long fibers addition). Mixture proportion in percentage (%) by weight.

Mixture ID	Rice husk	Marble dust	MSWI BA	Cement	Lime	Sand	Soil	Water	w/b (-)
1-A	–	–	–	11.00	–	18.78	46.22	24	2.18
2-A	–	–	–	11.00	–	22.78	46.22	20	1.81
3-A	1.41	–	–	9.59	–	18.78	46.22	24	2.50
4-A	1.41	–	–	9.59	–	22.78	46.22	20	2.09
5-A	–	2.75	–	8.25		22.78	46.22	20	2.42
6-A	–	–	2.75	8.25	–	22.78	46.22	20	2.42
7-A	–	–	–	–	11.00	18.78	46.22	24	2.18
8-A	–	–	–	–	11.00	22.78	46.22	20	1.81
9-A	1.41	–	–	–	9.59	18.78	46.22	24	2.50
10-A	1.41	–	–	–	9.59	22.78	46.22	20	2.09
11-A		2.75			8.25	18.78	46.22	24	2.91
12-A	–	–	2.75	–	8.25	18.78	46.22	24	2.91
13-A	–	2.75	–	–	8.25	22.78	46.22	20	2.42

Table 6
Second set of mixes (with long fibers addition). Mixture proportion in percentage (%) by weight.

Mixture ID	Fiber (0.5%)	Shredded Rice husk	Marble dust	Lime	Sand	Soil	Water	w/b (-)
1-B	–	1.375	1.375	8.25	22.78	46.22	20	2.42
2-B	Juta	1.375	1.375	8.25	22.78	45.72	20	2.42
3-B	Coconut	1.375	1.375	8.25	22.78	45.72	20	2.42
4-B	Sisal	1.375	1.375	8.25	22.78	45.72	20	2.42
5-B	Goat hair	1.375	1.375	8.25	22.78	45.72	20	2.42

7, 14, 28, and 56 days, divided by the initial length value [70]. Two replicates for each mix were tested, and all measurements were taken using an electronic caliber with sensitivity of up to 0.1 mm.

3. Results

Results in terms of mechanical strength, hardened density and shrinkage are presented in Tables 7 and 8 for the two sets of mixes, without and with long fibers. Recall that all the mixes were designed initially to be printed, trying to move from the least sustainable ones (with cement) to the ones with lime and other alternative binders, being more sustainable. In addition, Tables 7 and 8 indicate whether or not the mixtures are printable by marking them with "YES" for printable mixtures and "NO" for non-printed mixtures, based on the results of the empirical sac-a-poche test procedure. For each mix, other than the average value, the standard deviation (*st.dev.*) of the results is presented for both strength and density values. Instead, for the shrinkage property only the average result is reported, since only two samples were tested per this property. When not indicated, results were considered not reliable and for this reason, they were discarded.

3.1. First set of mixes: density, mechanical strength, shrinkage and printability

In terms of hardened density, the mixes display an average density of 1740 kg/m^3, with a limited dispersion of ± 82 kg/m^3. The main parameter that affects this property is the water dosage, whereas all the other variables have a limited influence. The highest density attained is 1835 kg/m^3 for the Mix 4-A, while Mix 7-A showed the lowest value, i.e. 1657 kg/m^3.

Concerning the mechanical strength, the first consideration that must be made is that, in general, the variable which impacts this property more is the water dosage, and thus the water/binder content, as expected (see Fig. 9a-b). This result clearly follows Abrams' law, which states that the compressive strength of a cement-based mix is inversely dependent on the water/cement ratio (or alternatively, water/binder ratio). Among the whole set of tested specimens, in the reference mixes cement used as binder performs better in terms of both compressive and flexural strength, with the best performance exhibited by the mix made with the lowest water content (Mix 2-A). The partial replacement of cement with rice husk (Mix 3-A and Mix 4-A), marble dust (Mix 5-A) and MSWI BA (Mix 6-A) lowers both the strength values, being the strength loss highest when the replacement ratio is maximum, despite of the water content in the mix. This behavior is expected because these materials provide very little hydraulic and pozzolanic behavior. The highest loss is observed when the MSWI BA replaces partly the cement, being up to more than 60% for the compressive strength value.

When natural lime is used as an alternative binder to the ordinary cement, again a reduction of the mechanical strength is observed, due to the noteworthy lower performance of lime than cement in terms of strength development. For Mix 7-A and Mix 8-A, both flexural and compressive strength are almost half than those of Mix 1-A and Mix 2-A, respectively. Interestingly, the partial substitution of lime with the other materials, i.e., rice husk (Mix 9-A and Mix 10-A), marble dust (Mix 11-A and Mix 13-A) and MSWI BA (Mix 10-A) does not lead always to a strength reduction. The maximum reduction is observed again when MSWI BA replaces the binder, but it is limited up to 7% and 25%, for the compressive and flexural strength values respectively. When the marble dust is used, instead, a strength increases varying between 5 and 20% is displayed, depending on the water content in the mix and on the analyzed strength parameter. This result is particularly useful to suggest us that the marble dust could be added to the sustainable 3DP mix similarly to a natural limestone filler, aiming to reduce the porosity of the hardened material thanks to its high fineness, which effect is maximized in a softer matrix such as that made with lime rather than with cement. Such effect is clearly visible in Fig. 10, which plots both the compressive (a) and flexural strength (values) of Mix 2-A and Mix 5-A made with cement, and Mix 8-A and Mix 13-A made with lime. Mix 2-A and Mix 5-A were compared in terms of their flexural and compressive strengths after marble dust was added to each. All the mortars have the same water dosage (20%), in one case (in blue) they represent the reference mix and in the other (in red) the binder is partially substituted by marble dust.

In terms of shrinkage, most of the mixes are characterized by a relatively high value of this property, higher than 1%. This is particularly true for the reference mixtures made with cement (Mix 1-A and Mix 2-A) and made with lime (Mix 7-A, Mix 8-A, Mix 11-A, Mix 12-A and Mix 13-A), being higher in those mixes with the highest water dosage (see Fig. 11a). The worst performance is however displayed when marble dust and MSWI BA substitute partially the binder, and in fact the

Table 7
Results for the mixtures belonging to the first set (without long fibers).

Mixture ID	Density (kg/m^3)	st. dev. (kg/m^3)	Flexural strength (MPa)	st. dev. (MPa)	Compressive strength (MPa)	st. dev. (MPa)	Shrinkage (%)	Printability
1-A	1670	19.53	0.30	0.02	0.85	0.02	1.45	No
2-A	1828	2.60	0.43	0.04	1.40	0.09	0.83	Yes
3-A	1660	23.87	0.19	0.02	0.50	0.04	0.31	No
4-A	1835	13.89	0.43	0.07	1.16	0.04	0.63	Yes
5-A	1820	6.51	0.23	0.01	0.57	0.01	–	Yes
6-A	1836	14.32	0.20	0.01	0.52	0.02	–	Yes
7-A	1657	6.94	0.20	0.01	0.45	0.01	1.86	Yes
8-A	1779	12.15	0.26	0.01	0.71	0.03	1.67	No
9-A	1607	10.42	0.17	0.01	0.39	0.00	1.30	Yes
10-A	1763	6.08	0.24	0.01	0.62	0.01	0.83	No
11-A	1725	18.66	0.22	0.02	0.54	0.01	2.50	No
12-A	1651	17.36	0.15	0.03	0.42	0.01	2.50	No
13-A	1794	10.85	0.28	0.02	0.78	0.01	2.50	No

Table 8
Results for the mixtures belonging to the second set (with long fibers).

Mixture ID	Density (kg/m^3)	st. dev. (kg/m^3)	Flexural strength (MPa)	st. dev. (MPa)	Compressive strength (MPa)	st. dev. (MPa)	Shrinkage (%)	Printability
1-B	1973	22.14	0.34	0.03	0.92	0.08	0.44	Yes
2-B	2038	24.31	0.42	0.03	0.98	0.10	0.64	Yes
3-B	1956	25.61	0.53	0.05	1.23	0.11	0.61	Yes
4-B	1964	18.66	0.56	0.02	1.26	0.06	0.33	Yes
5-B	2029	27.34	0.55	0.00	1.17	0.04	0.84	Yes

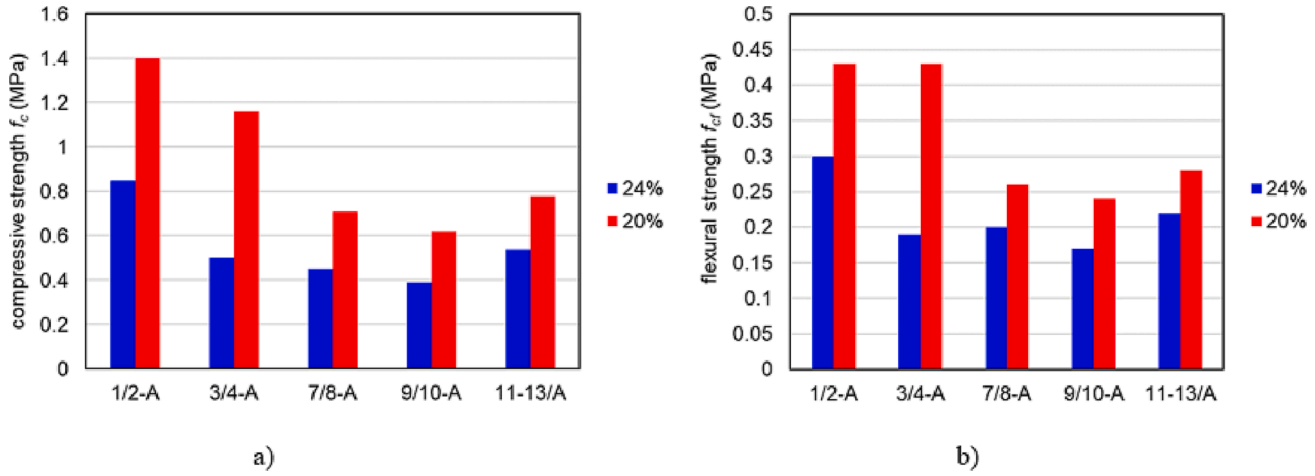

Fig. 9. Water dosage (%) effect on: a) compressive strength; b) flexural strength within the first set of tested mixes.

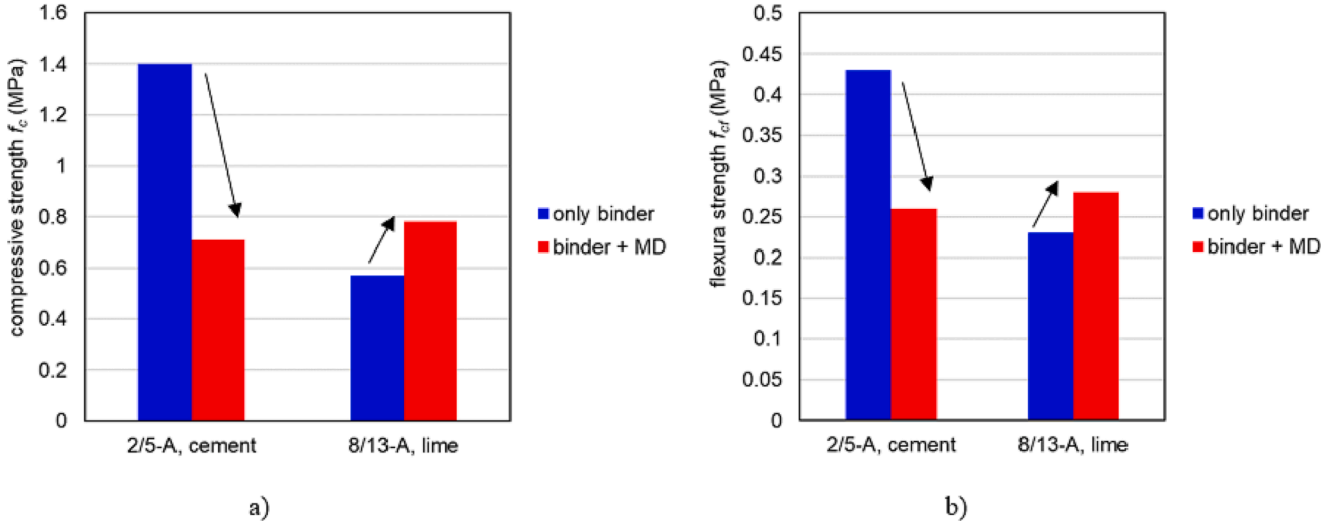

Fig. 10. Binder type and marble dust replacement effects on: a) compressive strength; b) flexural strength within the first set of tested mixes.

measured shrinkage increases up to 2.5%. However, for both the mixes made with cement and lime, and regardless of the water dosage, when the short fibers are used (i.e., rice husk), a positive enhancement of the shrinkage behavior is exhibited. Fig. 11b shows this effect for the mixes made with a water dosage of 24% as an indicative result. This evidence indicates us that, to optimize the mix, the content of fibers should be properly investigated to maximize their benefit, even those that have a limited length such as the rice husk ones. It is worth to recall that the shrinkage values observed here are very far from those typically shown by earth-materials, which can achieve even 20% when the clay content is particularly high, and the mix is not supplemented by the addition of sand and other stabilizers [71].

Finally, at this time, only a qualitative comment on printability outcomes is possible. It is feasible to establish clearly that an excess of water content causes the mix to be unable to stand out due to its own weight, resulting in generally poor results for the mixes with the maximum water dose, i.e., 24%. The best result for the mixes made with lime as binder is achieved when rice husk is used, whereas the addition of the other constituents, i.e., marble dust and MSWI BA, did not lead to a positive result.

All these results were considered when designing the second set of mixes, which results are discussed in the next Section. In fact, as shown in Table 6, all the new mixtures were casted with the lowest water dosage (20%), adopting the most sustainable binder (lime), maintaining a certain amount of marble dust that ensures to achieve higher mechanical strength in combination with lime, together with shredded rice husk, with the same aim. To limit the shrinkage values, short rice husk fibers were substituted with long ones, with a constant dosage of 0.5% in

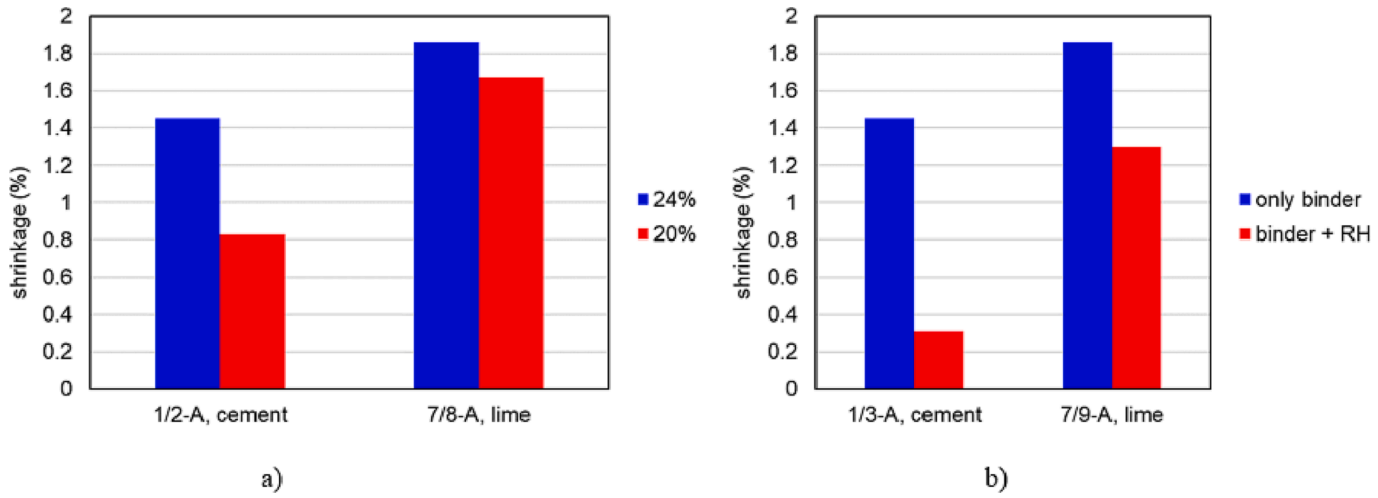

Fig. 11. Impact on shrinkage of: a) water dosage (%); b) rice husk addition on mixes with water dosage at 24%.

weight terms.

3.2. Second set of mixes: The effects of long fibers addition on mechanical strength, shrinkage and printability

Compared to the mixes of the first set (Mix 1A – Mix13A), the average hardened density of the mixtures of the second set (Mix 1B - Mix 5B) is slightly higher and equal to 1992 kg/m^3. In fact, these mixes were casted with the lowest water dosage only. For the same reason, also the dispersion of the results is lower and equal to ± 39 kg/m^3.

The reference mix for this new set is the Mix 1-B, which is the enhanced version of the Mix 13-A: in fact, it contains the same amount of lime, sand, soil and water dosage, while the filler content made originally of marble dust only is replaced partially, at 50%, with shredded rice husk particles. The effect of this first optimization on the mechanical strength is an enhancement of both compressive and flexural strength of + 18% and + 21%, respectively. Thus, we can comment on the impact of adding various types of long fibers considering that Mix 1-B is the optimal matrix containing lime without fibers.

For all the fiber types, an enhancement of the mechanical strength is observed, see Fig. 12a-b, for the compressive and flexural strength. Almost the same improvement was displayed when coconut, sisal fibers and goat hair were added to the mix at 0.5%, which varied between + 27% and + 37% for the compressive strength, and between + 56% and + 65% for the flexural strength. The strength enhancement is less pronounced when jute fibers are used. Fibers effects are noteworthy mostly influencing the behavior in tension of earth-based and cement-based materials, thanks to the well-known "bridge effect", which prevents cracks formation, limit their expansion and progression when the tensile stresses are increasing. However, the presence of fibers improves the toughness of earth-based materials too, making them less brittle, improving the ductility thanks to the extension of the softening branch after the load peak in their stress–strain curves, and consequently, leading them to absorb more energy. Such effects are visible, for a representative sample of each mix, in Fig. 13a-b, respectively for the behavior in compression and tension. Note that in compression the post-peak curve is characterized by a longer branch, with a significant improvement especially for Mix 3-B made with coconut fibers. For the other fiber types this is not visible clearly as the test was stopped quickly after the load peak was attained. Under flexure, instead, a first peak corresponding roughly to the unreinforced mix behavior (Mix 1-B) is visible for all the pastes. However, when fibers are added to the mix, a strength recovery is exhibited with a prolonged branch, showing the typical behavior of fiber-reinforced materials. The results obtained here are thus agreeing with other experimental observations on both earth- and cement-based materials, reinforced through natural fibers, even of different types (e.g., recycled carton pulp, bamboo pulp, sisal fibers) [72–73].

Concerning the shrinkage, the optimization of the mix was very successful to reduce the value of this property: in fact, compared to Mix 13-A, which had the highest shrinkage value equal to 2.5%, Mix 1-B is characterized by a significant lower deformation, equal to 0.44%. The

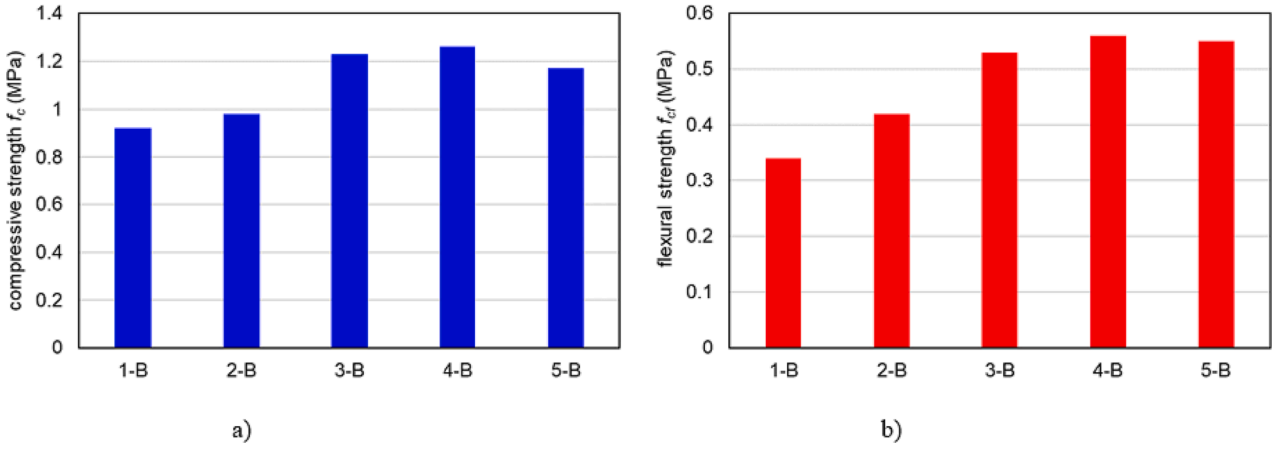

Fig. 12. Effects of fiber addiction on: a) compressive strength; b) flexural strength.

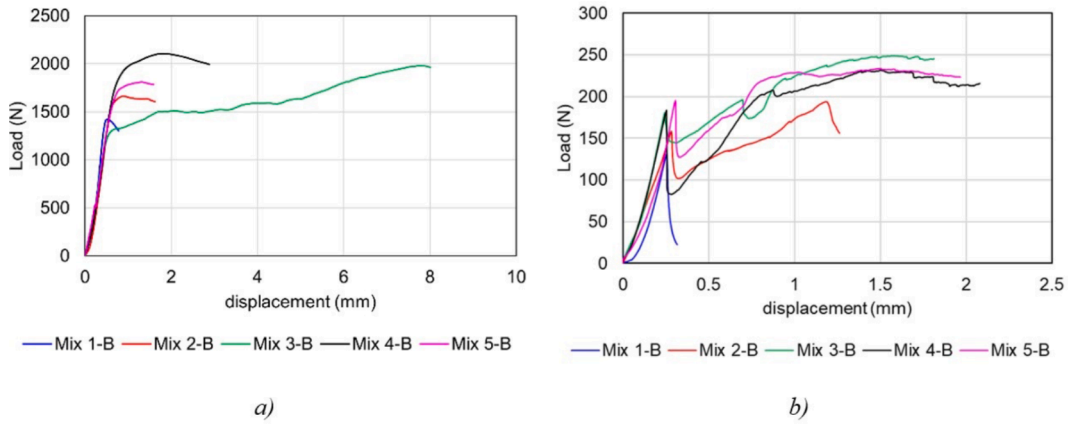

Fig. 13. Effects of fiber addiction on load–displacement curves under: a) compression; b) flexure.

addition of long fibers is not very effective to reduce more this value: in fact, within the second set of samples, only Mix 4-B, with sisal fibers, performed better. It is worth recalling that, among all the tested specimens, the best behavior is still displayed by Mix 3-A with rice husk: this result indicates that the presence of short fibers cannot be avoided at all in the final optimized mix, as it is very effective to control the shrinkage strain since the first curing days. This result may be due to the fact that small fibers allow to create a denser network of tensile-resistant components, that offer their strength opposed to the matrix contraction in a more efficient way than with longer fibers, which network would be more dispersed.

Lastly, concerning the qualitative evaluation of the printability of the mixes, all the mixes passed the sac-a-poche test, however, showing different performances. On one hand, the presence of the fibers made the mixes more difficult to work and extrud: the passing ability through the hole representing the extruder was the least when fibers have the highest diameter size (i.e., for the jute ones). This is due to the formation of some agglomerates, that overall, made the earth mix stiffer, requiring a higher pressure to be extruded. On the other hand, fibers addition made the mix more cohesive, thus each printed layer was more stable and was able to better sustain its own weight and that of the upper layers, without showing any bleeding phenomena.

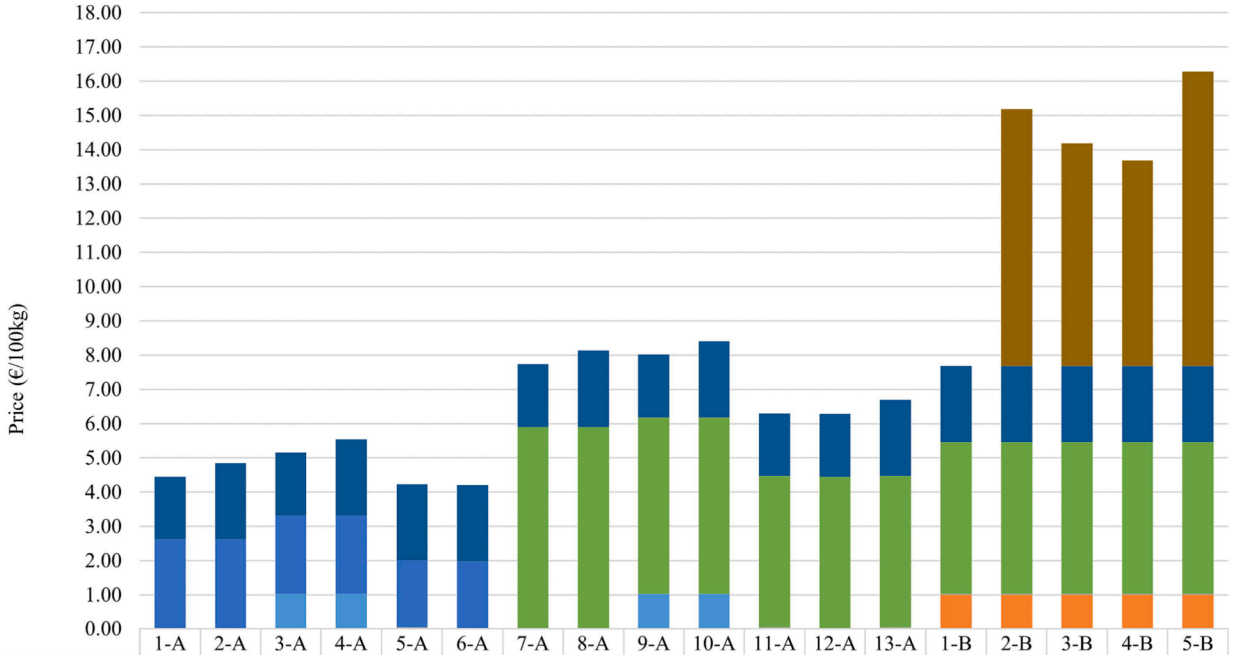

	1-A	2-A	3-A	4-A	5-A	6-A	7-A	8-A	9-A	10-A	11-A	12-A	13-A	1-B	2-B	3-B	4-B	5-B
Fibers															7.50	6.50	6.00	8.60
Sand	1.83	2.22	1.83	2.22	2.22	2.22	1.83	2.22	1.83	2.22	1.83	1.83	2.22	2.22	2.22	2.22	2.22	2.22
Natural Hydraulic Lime							5.90	5.90	5.15	5.15	4.43	4.43	4.43	4.43	4.43	4.43	4.43	4.43
Cement	2.62	2.62	2.28	2.28	1.96	1.96												
MSWI BA						0.02						0.02						
Marble dust					0.04						0.04		0.04	0.02	0.02	0.02	0.02	0.02
Shredded rice husk														1.01	1.01	1.01	1.01	1.01
Rice Husk			1.03	1.03					1.03	1.03								

Fig. 14. Economic evaluation of mixture prepared in this work.

3.3. Economic evaluation

The price of a building material strongly affects its diffusion in the market and, hence, its effective use. Fig. 14 shows an economic evaluation of the mixtures in € per 100 kg, based on the unit prices provided at Table 9. The estimation was carried out summarizing the unit cost per content for each component; the selling price (of the Italian market) was considered in this phase. No transportation costs are added to this evaluation, because they are strongly affected by the location. The contributions of water and natural soil are not considered, since they are locally available and their contribution to the final price can be neglected. In Table 9, it is possible to observe that the hydraulic lime and the fibers are the main contributors to the overall price. Recall that however increasing costs does not always lead to better performances of the mix. The lowest price of 4.20€/100 kg is characterizing Mix 6-A (with cement and MSWI BA, but no fibers), while the most expensive is mixture 5-B (with lime, shredded and not treated rice husk, marble dust and goat hair as long fiber), which cost is 16.28 €/100 kg. Among mixes containing long fibers, adding sisal allows obtaining the cheapest price, i.e. Mix 4-B price is 13.68 €/kg.

3.4. Multi-criteria efficiency evaluation

A multi-criteria convenience evaluation is useful to detect the most convenient mixture based on several parameters. In this work, a convenience study based on compressive strength, economic cost and embodied carbon is performed. The relationship between the involved parameters is provided by Equation (1):

$$EI = \frac{f_m(MPa)}{P\left(\frac{€}{kg}\right) x EC\left(\frac{kgCO_2eq}{kg}\right)} \quad (1)$$

where *EI* is the efficiency indicator, f_m is the compressive strength of the mixture, *P* is the economic price per kg, and *EC* is the embodied carbon per kg. In this approach, the input parameter for which a higher *EI* value is desirable is placed at the numerator (here, f_m), while at the denominator there are the price *P* and the embodied carbon *EC,* for which a lower value is needed. The input parameters and the results are shown at Table 10, where the compressive strength and the price are reported as calculated in previous sections. Instead, *EC* is calculated as it follows.

Embodied carbon is calculated in a simplistic way considering only the impact linked to the binder. In terms of carbon emissions, this choice can be justified by the negligible contribution to CO_2 emissions of the other constituents in comparison to the binder, furthermore, some materials, e.g. marble dust and MSWI BA, are by-products used "as-received", which impacts of the original productive chain are allocated to the main material only. The carbon footprint for an ordinary cement is considered equal to 930 $kgCO_2$/ton according to [74]. In this work a CEM II/B-LL was employed, which is composed of clinker in the range 65–79% and limestone filler for the remaining part. Considering an embodied carbon of 14.58 $kgCO_2$/ton for refined limestone powder [75], it is possible to calculate the CO_2 emissions for the cement employed in this work through proportion. According to the producer, a clinker percentage of 75% for this kind of cement can be considered reliable. Finally, the embodied carbon of Natural Hydraulic Lime is considered equal to 635 $kgCO_2$/ton as for [74].

This efficiency evaluation shows that, among the printable mixes, Mix 2-A is the most convenient. This fact demonstrates that the use of eco-friendly materials is not always justified from the economic and performance point of view. In this case, the mixtures containing cement attain higher performance with a reduced cost, which are not compensated for their higher environmental impact.

Anyway, in this case all involved parameters are considered with the same weight, alternative approaches can be employed varying the weight of each input of the formula.

Table 10
Multi-criteria efficiency evaluation.

Mixture ID	Compressive strength (MPa)	Price (€/kg)	Embodied carbon (kg CO2eq/kg)	Efficiency index (-)
1-A	0.85	0.045	0.07713	248
2-A	1.40	0.048	0.07713	375
3-A	0.50	0.051	0.06724	144
4-A	1.16	0.055	0.06724	311
5-A	0.57	0.042	0.05784	233
6-A	0.52	0.042	0.05784	214
7-A	0.45	0.077	0.06985	83
8-A	0.71	0.081	0.06985	125
9-A	0.39	0.080	0.06090	80
10-A	0.62	0.084	0.06090	121
11-A	0.54	0.063	0.05239	164
12-A	0.42	0.063	0.05239	128
13-A	0.78	0.067	0.05239	222
1-B	0.92	0.077	0.05239	229
2-B	0.98	0.152	0.05239	123
3-B	1.23	0.142	0.05239	166
4-B	1.26	0.137	0.05239	176
5-B	1.17	0.163	0.05239	137

4. Further developments

According to all the results shown in Section 3, a further optimization of the mix for a 3D printing test should be carried out, considering the following aspects:

- to adopt the most sustainable binder, i.e., lime;
- to increase the mechanical strength both in terms of compressive and tensile strength, i.e., adopting sustainable fillers, i.e., marble dust and shredded rice husk, and at the same time using partly some long fibers;
- to reduce the shrinkage, i.e., adopting a network of short and long fibers;
- to enhance the printability, i.e., maintaining the lowest water dosage to avoid bleeding phenomena, adopting a limited amount of long fibers to improve the passing ability during the extrusion but at the same time ensuring a sufficient cohesiveness of the mix.

To achieve the above targets, the optimization was carried out in terms of soil properties too, identifying the most suitable particles grading. Thus, the new optimized mix, which composition is not provided here due to intellectual property rights owned by the same authors, was printed to construct blocks with various geometry and different extrusion pattern on the WASP Crane 3D printer at the headquarters of WASP S.r.l. in Massa Lombarda, Italy. The main difference between the mix used here from the optimized one shown in Section 3 is in terms of the composition and grading of the soil, which was selected to guarantee higher performances. The blocks, in average, have a dimension of 100 × 35 × 50 cm. According to the producers, the

Table 9
Unit prices for each component for the economic evaluation.

	Rice Husk	Shredded rice husk	Marble dust	MSWI BA	Cement	Natural Hydraulic Lime	Sand	Juta	Coconut	Sisal	Goat hair
Unit price (€/kg)	0.73	0.73	0.02	0.01	0.24	0.54	0.10	15.00	13.00	12.00	17.20

particles maximum size should be 3 mm, the maximum length of the fibers should be 5 cm, and the workability of the mix should be maintained for at least 100 min. The mixes were casted in a concrete mixer with 120 L capacity and vertical axis, with the procedure already shown in Fig. 8, and then the printer was fed with the paste.

The Crane 3D printer as available in WASP S.r.l. has a printing area of 50 m^2, it consists of a 4.2 m long printer arm which is mounted on a truss column connected to a wide steel frame. While working, the printing arm is free to rotate around the column and hence, the extruder, which is free to translate along the arm, is able to print around a wide circular area. In this experimental work, the mixture was prepared separately, after which it was poured into the feeding hopper of the printer. The printing machine extrudes the material by exploiting synergically a system of screws and air pressure. For each printing material, it is important to optimize and adjust printing rate, and screws rotation speed. After pouring in the hopper, the mixture passes through the pipes, then the extruder, and arrives to the nozzle, finally. The nozzle is the last part in direct contact with the mixture, and therefore, it defines extrusion shape and dimension.

Fig. 15 shows the moment of the extrusion process and the final result of the work. The properties achieved, in terms of mechanical strength, are 11.04 MPa and 1.26 MPa of compressive and flexural strength, respectively; in terms of shrinkage, it was possible to limit this value below 0.5%. For this material, a printing rate of about 10 cm/s was employed on a circular nozzle with 30 mm of diameter.

5. Conclusions

This work shows the results of an experimental work, carried out through different optimization steps, that allowed to design a new sustainable earth-based mix for 3D printing. Different materials were tested and their influence on the properties that need to be considered when designing this kind of materials are discussed. Particularly, compressive and tensile strength, shrinkage strains and printability were considered as fundamental aspects. The main conclusions that were obtained are the following:

- The mix with the best mechanical properties reached 0.43 MPa and 1.40 MPa of flexural and compressive strength, respectively. Among the mixtures containing lime as binder, the highest compressive strength was 1.26 MPa. The optimized mixture prepared for the real-scale 3D printing reached 11.04 MPa and 1.26 MPa of compressive and flexural strength, respectively.
- In terms of hardened density, the mixes of the first set display an average density of 1740 kg/m^3, with a limited dispersion of ± 82 kg/m^3. The main parameter that affects this property is the water dosage, whereas all the other variables have a limited influence. Mixture 5-B showed the maximum density, equal to 2029 kg/m^3, while mix 7-A attained the value of 1651 kg/m^3 resulting as the minimum.
- The partial replacement of cement with rice husk, marble dust and municipal waste incinerator bottom ash (MWI BA) is always detrimental: the highest loss was recorded for MSWI BA, being more than 60% for the compressive strength. Differently, the partial substitution of lime with other materials does not always lead to a strength reduction. For instance, when marble dust was used, a strength increase between 5 and 20 % is recorded, depending on the water content.
- Water dosage significantly affects mechanical strength development and the potential development of bleeding phenomena, thus this parameter should be properly controlled. In this work, a 20% water dosage was found to be optimum to design a 3DP mix.
- When natural lime is used as binder, the addition of fillers allows to improve the mechanical strength and to make the fresh mix more cohesive and stiffer, thus also improving the ability of each printed layer to sustain the loads in the fresh state. Here, the adoption of marble dust and shredded rice husk were effective to achieve this goal.
- Careful consideration should be given to the selection of soil type and particle size in order to enhance the mix mechanical qualities. Additionally, the incorporation of long fibers is efficient in enhancing the mix tensile behavior.
- Shrinkage is also influenced by soil type, water dosage and presence of fibers. First, a well-balanced mix of clay and sand allows to limit strain developments; then, extra water induce rapid strain development; lastly, short fibers were found to be more efficient than longer ones to reduce the contraction of the mixes. The maximum shrinkage recorded was 2.5% when marble dust and MSWI BA substitute partially the binder.
- The lowest price of 4.20€/100 kg is relative to Mix 6-A, while the most expensive is mixture 5-B, which cost is 16.28 €/100 kg. Among mixes containing long fibers, sisal allows obtaining the cheapest one, i.e. Mix 4-B.
- The efficiency evaluation demonstrates that it is possible to produce low-price earth-based materials with a reduced carbon footprint: mixture containing lime as binder and sisal as long fibers allows attaining a compressive strength of 1.26 MPa, embodied carbon of

a) b)

Fig. 15. 3DP blocks made with the optimized mix: a) extrusion process; b) final blocks.

about 0.05239 $kgCO_2eq/kg$ with a selling price of 0.137€/kg, being the most efficient between the mixes with lowest environmental impact. However, mix 2-A seems to be the most efficient among all.

The printing test in a real scale 3D printer for building constructions has demonstrated the feasibility of designing printable mixes made with earth-based materials and recycled components, attaining high mechanical strength and low shrinkage deformation. Further works will be carried out by the authors to further optimize the mixing procedure and to provide proper composition limits for each constituent, to guarantee a more controlled design process of this kind of materials. Further, since organic fibers are used, durability issues will be investigated, due to the possibility of their deterioration in alkaline environment.

CRediT authorship contribution statement

Flora Faleschini: Conceptualization, Investigation, Methodology, Formal analysis, Supervision. **Daniel Trento:** Investigation, Formal analysis. **Maryam Masoomi:** Investigation, Formal analysis. **Carlo Pellegrino:** Resources, Project administration. **Mariano Angelo Zanini:** Conceptualization, Methodology, Project administration, Supervision.

Declaration of Competing Interest

The authors declare that they have no known competing financial interests or personal relationships that could have appeared to influence the work reported in this paper.

Data availability

Data will be made available on request.

Acknowledgments

This work has been done under a POR FESR 2014-2020 project named “Hybrid Sustainable Worlds”, action 1.1.4 DGR 822/2020, funded by Regione Veneto to the RIR Venetian Green Building. Thus, the authors would like to express their acknowledgment to all the partners of the project, particularly to Fablab Venezia Srl who coordinated the TG 5.1, and all the other participants: Green Prefab, La.So.Le, Iconia Ingegneria Civile, Fattori srl, Crea Ecoliving, University IUAV Venice. A special thank is also provided to WASP S.r.l. for their availability to test our mix, giving us the possibility to use their technology for a real-scale project on 3DP prefabrication.

Appendix A. Supplementary data

Supplementary data to this article can be found online at https://doi.org/10.1016/j.conbuildmat.2023.132496.

References

[1] REN21 (2022), Renewables 2022 Global Status.
[2] G.L.F. Benachio, M.d.C.D. Freitas, S.F. Tavares, Circular economy in the construction industry: a systematic literature review, J. Clean. Prod. 260 (2020), 121046.
[3] M. Carsana, F. Canonico, L. Bertolini, Corrosion resistance of steel embedded in sulfoaluminate-based binders, Cem. Concr. Compos. 88 (2018) 211–219.
[4] R. Trauchessec, J.M. Mechling, A. Lecomte, A. Roux, B. Le Rolland, Hydration of ordinary Portland cement and calcium sulfoaluminate cement blends, Cem. Concr. Compos. 56 (2015) 106–114.
[5] E. Gartner, T. Sui, Alternative cement clinkers, Cem. Concr. Res. 114 (2018) 27–39.
[6] B. Singh, G. Ishwarya, M. Gupta, S.K. Bhattacharyya, Geopolymer concrete: A review of some recent developments, Constr. Build. Mater. 85 (2015) 78–90.
[7] A.M. Maglad, O. Zaid, M.M. Arbili, G. Ascensão, A.A. Şerbănoiu, C.M. Grădinaru, R.M. García, S.M.A. Qaidi, F. Althoey, J. de Prado-Gil, A study on the properties of geopolymer concrete modified with nano graphene oxide, Buildings 12 (8) (2022) 1066.
[8] G. Ascensão, M. Marchi, M. Segata, F. Faleschini, Y. Pontikes, Reaction kinetics and structural analysis of alkali activated Fe–Si–Ca rich materials, J. Clean. Prod. 246 (2020), 119065.
[9] V. Shobeiri, B. Bennett, T. Xie, P. Visintin, A comprehensive assessment of the global warming potential of geopolymer concrete, J. Clean. Prod. 297 (2021), 126669.
[10] C. Gunasekara, D. Law, S. Bhuiyan, S. Setunge, L. Ward, Chloride induced corrosion in different fly ash based geopolymer concretes, Constr. Build. Mater. 200 (2019) 502–513.
[11] M. Etxeberria, A.R. Marí, E. Vázquez, Recycled aggregate concrete as structural material, Mater. Struct. 40 (5) (2007) 529–541.
[12] L. Evangelista, J.M.C.L. De Brito, Durability performance of concrete made with fine recycled concrete aggregates, Cem. Concr. Compos. 32 (1) (2010) 9–14.
[13] B. González-Fonteboa, I. González-Taboada, D. Carro-López, F. Martínez-Abella, Influence of the mixing procedure on the fresh state behaviour of recycled mortars, Constr. Build. Mater. 299 (2021), 124266.
[14] V. Revilla-Cuesta, M. Skaf, R. Serrano-López, V. Ortega-López, Models for compressive strength estimation through non-destructive testing of highly self-compacting concrete containing recycled concrete aggregate and slag-based binder, Constr. Build. Mater. 280 (2021), 122454.
[15] V. Revilla-Cuesta, L. Evangelista, J. de Brito, M. Skaf, J.M. Manso, Shrinkage prediction of recycled aggregate structural concrete with alternative binders through partial correction coefficients, Cem. Concr. Compos. 129 (2022), 104506.
[16] F. Faleschini, M.A. Fernández-Ruíz, M.A. Zanini, K. Brunelli, C. Pellegrino, E. Hernández-Montes, High performance concrete with electric arc furnace slag as aggregate: mechanical and durability properties, Constr. Build. Mater. 101 (2015) 113–121.
[17] F. Faleschini, P. Bragolusi, M.A. Zanini, P. Zampieri, C. Pellegrino, Experimental and numerical investigation on the cyclic behavior of RC beam column joints with EAF slag concrete, Eng. Struct. 152 (2017) 335–347.
[18] E.K. Anastasiou, I. Papayianni, M. Papachristoforou, Behavior of self compacting concrete containing ladle furnace slag and steel fiber reinforcement, Mater. Des. 59 (2014) 454–460.
[19] G. Fares, A.I. Al-Negheimish, F.M. Al-Mutlaq, A.M. Alhozaimy, M. Iqbal Khan, Effect of freshly produced electric arc-furnace dust and chloride-free chemical accelerators on concrete performance, Constr. Build. Mater. 274 (2021), 121832.
[20] A. Bhardwaj, P. Kumar, S. Siddique, A. Shukla, Comprehensive review on utilization of waste foundry sand in concrete, Eur. J. Environ. Civ. Eng. (2022) 1–32.
[21] D. Hou, D.i. Wu, X. Wang, S. Gao, R. Yu, M. Li, P. Wang, Y. Wang, Sustainable use of red mud in ultra-high performance concrete (UHPC): Design and performance evaluation, Cem. Concr. Compos. 115 (2021), 103862.
[22] I. Kothman, N. Faber, How 3D printing technology changes the rules of the game: Insights from the construction sector, J. Manuf. Technol. Manag. 27 (7) (2016) 932–943.
[23] T.T. Le, S.A. Austin, S. Lim, R.A. Buswell, A.G. Gibb, T. Thorpe, Mix design and fresh properties for high-performance printing concrete, Mater. Struct. 45 (8) (2012) 1221–1232.
[24] P. Wu, J. Wang, X. Wang, A critical review of the use of 3-D printing in the construction industry, Autom. Constr. 68 (2016) 21–31.
[25] N. Roussel, Rheological requirements for printable concretes, Cem. Concr. Res. 112 (2018) 76–85.
[26] R.J.M. Wolfs, F.P. Bos, T.A.M. Salet, Hardened properties of 3D printed concrete: The influence of process parameters on interlayer adhesion, Cem. Concr. Res. 119 (2019) 132–140.
[27] G.M. Moelich, J. Kruger, R. Combrinck, Plastic shrinkage cracking in 3D printed concrete, Compos. B Eng. 200 (2020), 108313.
[28] B. Zareiyan, B. Khoshnevis, Effects of interlocking on interlayer adhesion and strength of structures in 3D printing of concrete, Autom. Constr. 83 (2017) 212–221.
[29] A. Kazemian, B. Khoshnevis, Real-time extrusion quality monitoring techniques for construction 3D printing, Constr. Build. Mater. 303 (2021), 124520.
[30] M. van den Heever, A. du Plessis, J. Kruger, G. van Zijl, Evaluating the effects of porosity on the mechanical properties of extrusion-based 3D printed concrete, Cem. Concr. Res. 153 (2022), 106695.
[31] J. Xiao, G. Ji, Y. Zhang, G. Ma, V. Mechtcherine, J. Pan, L.i. Wang, T. Ding, Z. Duan, S. Du, Large-scale 3D printing concrete technology: Current status and future opportunities, Cem. Concr. Compos. 122 (2021), 104115.
[32] M. Gomaa, W. Jabi, V. Soebarto, Y.M. Xie, Digital manufacturing for earth construction: a critical review, J. Clean. Prod. 338 (2022) 130630.
[33] M. Gomaa, W. Jabi, A. Veliz Reyes, V. Soebarto, 3D printing system for earth-based construction: case study of cob, Autom. Constr. 124 (2021), 103577.
[34] NZS D4298: 2020. Earth buildings not requiring specific engineering design.
[35] New Mexico Earthen Building Code: 2015. Part 4.
[36] https://www.3dwasp.com/en/about-us/ (last access: 04/12/2022).
[37] D. Arduin, L.R. Caldas, R.D.L.M. Paiva, F. Rocha, Life cycle assessment (LCA) in earth construction: a systematic literature review considering five construction techniques, Sustainability 14 (20) (2022) 13228.
[38] F. Hadji, N. Ihaddadene, R. Ihaddadene, A. Betga, A. Charick, P.O. Logerais, Thermal conductivity of two kinds of earthen building materials formerly used in Algeria, J. Build. Eng. 32 (2020), 101823.
[39] L. Zhang, A. Gustavsen, B.P. Jelle, L. Yang, T. Gao, Y. Wang, Thermal conductivity of cement stabilized earth blocks, Constr. Build. Mater. 151 (2017) 504–511.
[40] L. Keefe, Earth building: methods and materials, repair and conservation, Routledge, 2012.

[41] E. Hamard, B. Cazacliu, A. Razakamantsoa, J.C. Morel, Cob, a vernacular earth construction process in the context of modern sustainable building, Build. Environ. 106 (2016) 103–119.
[42] H. Alhumayani, M. Gomaa, V. Soebarto, W. Jabi, Environmental assessment of large-scale 3D printing in construction: a comparative study between cob and concrete, J. Clean. Prod. 270 (2020), 122463.
[43] B. Panda, S. Ruan, C. Unluer, M.J. Tan, Improving the 3D printability of high volume fly ash mixtures via the use of nano attapulgite clay, Compos. B Eng. 165 (2019) 75–83.
[44] Veliz Reyes, A. A., Gomaa, M., Chatzivasileiadi, A., Jabi, W., & Wardhana, N. M. (2018). Computing craft: Early development of a robotically-supported cob 3D printing system. In *eCAADe 2018: Computing for a better tomorrow (Vol 1)*. Faculty of Civil Engineering, Architecture and Environmental Engineering, Lodz University of Technology.
[45] A. Alqenaee, A. Memari, Experimental study of 3D printable cob mixtures, Constr. Build. Mater. 324 (2022), 126574.
[46] E. Ferretti, M. Moretti, A. Chiusoli, L. Naldoni, F. De Fabritiis, M. Visonà, Rice-husk shredding as a means of increasing the long-term Mechanical properties of earthen mixtures for 3D printing, Materials 15 (3) (2022) 743.
[47] A. Perrot, D. Rangeard, E. Courteille, 3D printing of earth-based materials: Processing aspects, Constr. Build. Mater. 172 (2018) 670–676.
[48] G. Silva, R. Ñañez, D. Zavaleta, V. Burgos, S. Kim, G. Ruiz, M.A. Pando, R. Aguilar, J. Nakamatsu, Eco-friendly additive construction: analysis of the printability of earthen-based matrices stabilized with potato starch gel and sisal fibers, Constr. Build. Mater. 347 (2022), 128556.
[49] J.G. Sanjayan, B. Nematollahi, M. Xia, T. Marchment, Effect of surface moisture on inter-layer strength of 3D printed concrete, Constr. Build. Mater. 172 (2018) 468–475.
[50] E. Hosseini, M. Zakertabrizi, A.H. Korayem, G. Xu, A novel method to enhance the interlayer bonding of 3D printing concrete: An experimental and computational investigation, Cem. Concr. Compos. 99 (2019) 112–119.
[51] T. Marchment, J. Sanjayan, M. Xia, Method of enhancing interlayer bond strength in construction scale 3D printing with mortar by effective bond area amplification, Mater. Des. 169 (2019), 107684.
[52] C.S. Tang, B. Shi, C. Liu, W.B. Suo, L. Gao, Experimental characterization of shrinkage and desiccation cracking in thin clay layer, Appl. Clay Sci. 52 (1–2) (2011) 69–77.
[53] EN 197–1:2011, Cement Composition, specifications and conformity criteria for common cements, CEN, Comité européen de normalization, Brussels, Belgium, 2011, p. 52.
[54] ASTM D6913/D6913m-17, Standard Test Methods for Particle-Size Distribution (Gradation) of Soils Using Sieve Analysis, ASTM Int, West Conshohocken, PA, 2017.
[55] ASTM D7928–16, Standard Test Method for Particle-Size Distribution (Gradation) of Fine-Grained Soils Using the Sedimentation (Hydrometer) Analysis, ASTM Int, West Conshohocken, PA, 2016.
[56] ASTM D4318–17e1, Standard Practice for Classification of Soils for Engineering Purposes (Unified Soil Classification System), ASTM Int, West Conshohocken, PA, 2020.
[57] EN 459–1: 2015, Building lime - part 1: definitions, specifications and conformity criteria, CEN, Comité européen de normalization, Brussels, Belgium, 2015.
[58] R. Jauberthie, F. Rendell, S. Tamba, I. Cisse, Origin of the pozzolanic effect of rice husks, Constr. Build. Mater. 14 (8) (2000) 419–423.
[59] L. Restuccia, G.A. Ferro, D. Suarez-Riera, A. Sirico, P. Bernardi, B. Belletti, A. Malcevschi, Mechanical characterization of different biochar-based cement composites, Procedia Struct. Integrity 25 (2020) 226–233.
[60] R. Jauberthie, F. Rendell, S. Tamba, I.K. Cissé, Properties of cement—rice husk mixture, Constr. Build. Mater. 17 (4) (2003) 239–243.
[61] Amziane, S., & Collet, F. (Eds.). (2017). Bio-aggregates based building materials: state-of-the-art report of the RILEM Technical Committee 236-BBM (Vol. 23). *Springer*.
[62] A. Antunes, P. Faria, V. Silva, A. Brás, Rice husk-earth based composites: A novel bio-based panel for buildings refurbishment, Constr. Build. Mater. 221 (2019) 99–108.
[63] N. Johar, I. Ahmad, A. Dufresne, Extraction, preparation and characterization of cellulose fibres and nanocrystals from rice husk, Ind. Crop. Prod. 37 (1) (2012) 93–99.
[64] F. Faleschini, K. Toska, M.A. Zanini, F. Andreose, A.G. Settimi, K. Brunelli, C. Pellegrino, Assessment of a Municipal Solid Waste Incinerator Bottom Ash as a Candidate Pozzolanic Material: Comparison of Test Methods, Sustainability 13 (16) (2021) 8998.
[65] En 1097–6:2013., Tests for mechanical and physical properties of aggregates - Part 6: Determination of particle density and water absorption, CEN, Comité européen de normalization, Brussels, Belgium, 2013.
[66] ASTM E2392-310, “Standard Guide for Design pf Earthen Wall Building Systems”, American Society for Testing and Materials, 1-10.
[67] M. Palumbo, F. McGregor, A. Heath, P. Walker, The influence of two crop by-products on the hygrothermal properties of earth plasters, Building and Evironment 113 (2016) 108–116.
[68] En 1015–11:2019, Methods of test for mortar for mansonry - Part 6: Determination of flexural and compressive strength of hardened mortar, CEN, Comité européen de normalization, Brussels, Belgium, 2019.
[69] EN 12617-4:2002 09 01 - Products and systems for the protection and repair of concrete structures - Test methods - Part 4: Determination of shrinkage and expansion. *CEN, Comité européen de normalization*, Brussels, Belgium.
[70] EN 12390–16, Testing hardened concrete - Part 16: Determination of the shrinkage of concrete, CEN, Comité européen de normalization, Brussels, Belgium, 2019.
[71] M. Pedergnana, S.T. Elias-Ozkan, Impact of various sands and fibres on the physical and mechanical properties of earth mortars for plasters and renders, Constr. Build. Mater. 308 (2021), 125013.
[72] T.T. Stanislas, J.F. Tendo, R.S. Teixeira, E.B. Ojo, G.C. Komadja, M. Kadivar, H. S. Junior, Effect of cellulose pulp fibres on the physical, mechanical, and thermal performance of extruded earth-based materials, J. Build. Eng. 39 (2021), 102259.
[73] M. Benzerara, S. Guihéneuf, R. Belouettar, A. Perrot, Combined and synergic effect of algerian natural fibres and biopolymers on the reinforcement of extruded raw earth, Constr. Build. Mater. 289 (2021), 123211.
[74] E.R. Grist, K.A. Paine, A. Heath, J. Norman, H. Pinder, The environmental credentials of hydraulic lime-pozzolan concretes, J. Clean. Prod. 93 (2015) 26–37.
[75] A.L.M.V. Rodrigues, Á.Á.F. Mendes, V. Gomes, A.F. Battagin, M.R.M. Saade, M. G. Da Silva, Environmental and mechanical evaluation of blended cements with high mineral admixture content, Front. Mater. 9 (880986) (2022) 1–11.